Inorganic Chemistry

Article

pubs.acs.org/IC

Tetradecanuclear Iron(III)-Oxo Nanoclusters Stabilized by Trilacunary Heteropolyanions

Masooma Ibrahim,[†,▽] Ali Haider,[†] Yixian Xiang,[†] Bassem S. Bassil,[†,‡] Akina M. Carey,[†] Lisa Rullik,[†] Geoffrey B. Jameson,[#] Floriant Doungmene,[§] Israël M. Mbomekallé,*[,§] Pedro de Oliveira,[§] Valeriu Mereacre,[∥] George E. Kostakis,[△] Annie K. Powell,*[,∥,⊥] and Ulrich Kortz*[,†]

[†]Department of Life Sciences and Chemistry, Jacobs University, P.O. Box 750 561, 28725 Bremen, Germany

[‡]Department of Chemistry, Faculty of Sciences, University of Balamand, P.O. Box 100, Tripoli, Lebanon

[#]Institute of Fundamental Sciences, Massey University, Tennent Drive, Palmerston North 4442, New Zealand

[§]Equipe d'Electrochimie et de Photoélectrochimie, Laboratoire de Chimie-Physique, Université Paris-Sud, UMR 8000 CNRS, Orsay F-91405, France

[∥]Institute of Inorganic Chemistry, Karlsruhe Institute of Technology (KIT), Engesserstrasse 15, 76131 Karlsruhe, Germany

[△]Department of Chemistry, School of Life Sciences, University of Sussex, Brighton BN1 9QJ, United Kingdom

[⊥]Institute of Nanotechnology, Karlsruhe Institute of Technology (KIT), Hermann-von-Helmholtz Platz 1, 76344 Eggenstein-Leopoldshafen, Germany

Supporting Information

ABSTRACT: The tetrameric, multi-Fe^{III}-containing polyoxotungstates $[Fe_{14}O_6(OH)_{13}(P_2W_{15}O_{56})_4]^{31-}$ (**1**) and $[Na_2Fe_{14}(OH)_{12}(PO_4)_4(A\text{-}\alpha\text{-}XW_9O_{34})_4]^{20-}$ (X = Si^{IV} (**2**), Ge^{IV} (**3**)) have been successfully synthesized under conventional reaction conditions in aqueous, slightly acidic (**1**), or basic (**2** and **3**) media. Polyanions **1**-**3** were characterized in the solid state by single-crystal X-ray diffraction, IR spectroscopy, thermogravimetric analysis, and magnetic studies, and in solution by electrochemistry.

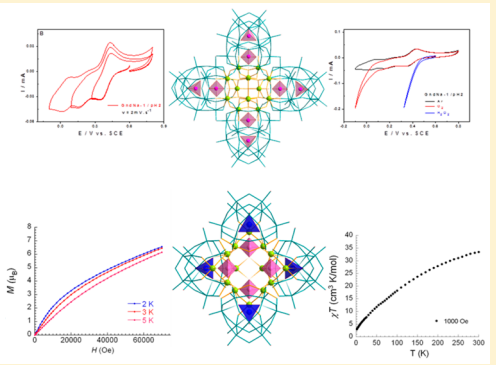

INTRODUCTION

Polyoxometalates (POMs) of early transition metals in high oxidation states (e.g., V^V, Mo^{VI}, W^{VI}) are a large and rapidly expanding family of molecular metal-oxo complexes.[1] The formation mechanism of this class of compounds is often not well-understood and is commonly described as self-assembly, with the template effect often playing an important role.[1,2] A considerable number of lacunary POMs (missing one or more W^{VI} and exposing coordinatively unrequited oxo groups) such as $[A\text{-}\alpha\text{-}PW_9O_{34}]^{9-}$, $[\gamma\text{-}PW_{10}O_{36}]^{7-}$, $[\alpha\text{-}PW_{11}O_{39}]^{7-}$, $[H_2P_2W_{12}O_{48}]^{12-}$, $[P_2W_{15}O_{56}]^{12-}$, $[P_2W_{17}O_{61}]^{10-}$, $[H_7P_8W_{48}O_{184}]^{33-}$, $[A\text{-}\alpha\text{-}XW_9O_{34}]^{10-}$ (X = Si, Ge), $[\gamma\text{-}XW_{10}O_{36}]^{8-}$ (X = Si, Ge), and $[XW_{11}O_{39}]^{8-}$ (X = Si, Ge) can be synthesized by either one- or two-step processes in high yield according to reported standardized methods.[2] By virtue of their exposed oxo ligands, these lacunary POMs constitute a large class of rigid diamagnetic multidentate inorganic ligands that can encapsulate a wide range of transition metal ions resulting in multi-transition metal aggregates.[3,4]

The growing interest in the field of polynuclear transition metal-containing POMs is due to their various chemical and physical properties, making them potential magnetic, catalytic, and optical materials, among others.[3] The literature contains, in particular, many examples of magnetic transition metal-containing POMs, which have been discussed recently in two reviews.[4] Even though the synthetic approaches for transition metal-containing POMs seem to be relatively straightforward, it is always a challenge to isolate in phase-pure form and thoroughly characterize new compounds with interesting physiochemical properties. It is due to various reaction conditions such as pH, type of solvent, buffer capacity, ionic strength, countercations, presence of auxiliary ligands, etc., that the synthesis of such compounds requires a considerable level of systematic screening of various conditions.[4]

POMs containing polynuclear iron(III)-oxo aggregates are of particular interest in bioinorganic chemistry and materials science.[5] As an example, in the bioinorganic field, there is a special need for modeling the structure and function of the iron/oxide/hydroxide core of the iron storage protein, ferritin, which incorporates up to 4500 Fe centers.[5a,e] On the other hand, high-

Received: January 19, 2015
Published: June 12, 2015

DOI: 10.1021/acs.inorgchem.5b00124
Inorg. Chem. 2015, 54, 6136−6146

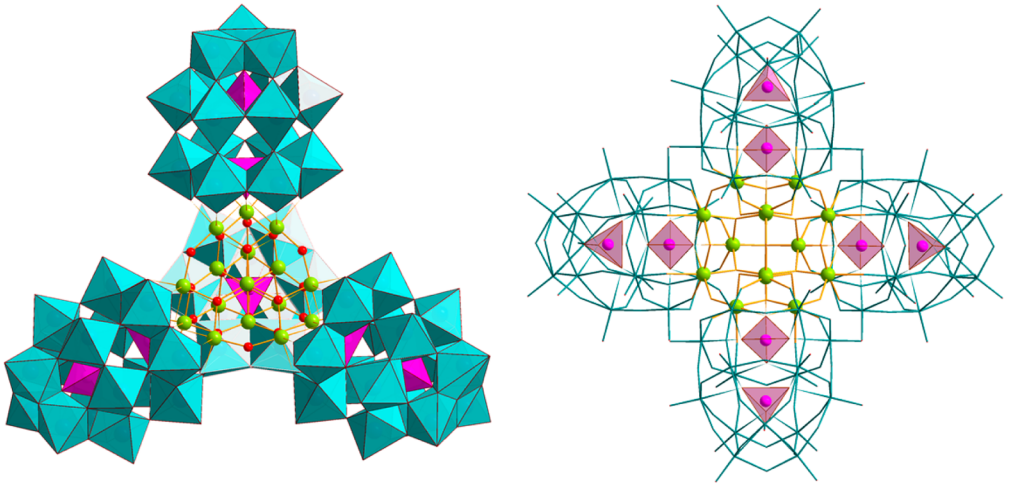

Figure 1. Combined polyhedral/ball-and-stick representation of **1**. Color code: WO_6 octahedra (aqua), Fe (lime), PO_4 (pink), O (red).

spin iron(III) ions have five unpaired electrons (d^5, $S = {}^5/_2$) and generally show strong, antiferromagnetic exchange interactions when oxo bridges are present.[5b−d] Nevertheless, iron-based compounds can sometimes have large ground-state spin (S) values and even show single-molecule magnet (SMM) behavior.[5f] Also, several iron(III)-containing POMs with spectacular structures have been isolated including species with up to 30 Fe^{III} centers.[6] For example, the remarkable compound $[\{(Mo^{VI})Mo^{VI}_5O_{21}L_6\}_{12}\{Fe(H_2O)L\}_{30}]$ (L = $H_2O/CH_3COO^-/Mo_2O_{8/9}^{n-}$) with icosahedral symmetry, published by Müller and co-workers, is composed of 12 pentagonal $\{(Mo^{VI})Mo^{VI}_5\}$ fragments connected with each other via Fe^{III} linkers.[6a] Later, Gouzerh's group reported two iron-containing phosphotungstates, $[H_{55}P_8W_{49}Fe_{27}O_{248}]^{26-}$ and $[H_4P_2W_{12}Fe_9O_{56}(OAc)_7]^{6-}$.[6e] The former assembly can be described as a Wells−Dawson superstructure consisting of four $\{P_2W_{12}Fe_6\}$ subunits connected via three Fe−O−Fe bridges to an encapsulated $\{Fe_4O_6\}$ core, while the latter is constructed from a hexavacant $\{P_2W_{12}\}$ anion filled with six iron atoms on the vacant sites, forming a hexasubstituted Wells−Dawson entity $\{P_2W_{12}Fe_6\}$, which in return supports three additional iron atoms. The coordination spheres of the Fe^{III} centers are in turn completed by acetate ligands. Another "iron(III)-rich" tungstophosphate, $[P_8W_{48}O_{184}Fe_{16}(OH)_{28}(H_2O)_4]^{20-}$ was documented in 2008, where a $\{Fe_{16}(OH)_{28}(H_2O)_4\}^{20+}$ nanocluster is grafted inside the crown-shaped $[H_7P_8W_{48}O_{184}]^{33-}$ precursor.[6f] Many tetrameric, iron-containing assemblies based on Keggin and Wells-Dawson type trilacunary ligands have also been reported in the literature.[6g−l]

Over the years, by studying different POM ligands under new reaction conditions, we have reported many multinuclear transition metal-containing POMs with interesting physical and chemical properties.[3c,f,k,7e,f,g] For example, the role of phosphate as coligand in POM synthesis is well-known, and several examples have been reported.[3c,f,k,7e,f,g] Here it is important to mention also that the role of carboxylate-based ligands in formation of multinuclear transition metal complexes, especially in iron-containing compounds, is well-known.[8,9] Following this approach we have now succeeded in preparing the three tetrameric assemblies, the 60-tungsto-8-phosphate $[Fe_{14}(OH)_{13}O_6\{\alpha\text{-}P_2W_{15}O_{56}\}_4]^{31-}$ (**1**), the 36-tungsto-4-silicate $[Na_2Fe_{14}(OH)_{12}(PO_4)_4(A\text{-}\alpha\text{-}SiW_9O_{34})_4]^{20-}$ (**2**), and the 36-tungsto-4-germanate $[Na_2Fe_{14}(OH)_{12}(PO_4)_4(A\text{-}\alpha\text{-}GeW_9O_{34})_4]^{20-}$ (**3**), all containing 14 iron(III) centers (Figures 1−6). The title compounds were synthesized by the interaction of Fe^{III} ions with the Wells−Dawson type trilacunary ligand $[\alpha\text{-}P_2W_{15}O_{56}]^{12-}$ and Keggin type trilacunary ligand $[A\text{-}\alpha\text{-}XW_9O_{34}]$ (X = Si^{IV}, Ge^{IV}) under normal bench conditions and in the presence of acetate and phosphate as coligands, respectively. The hydrated salts of **1**-**3** were characterized in the solid state by IR spectroscopy, single-crystal X-ray diffraction, thermogravimetric and elemental analysis, as well as magnetic susceptibility measurements.

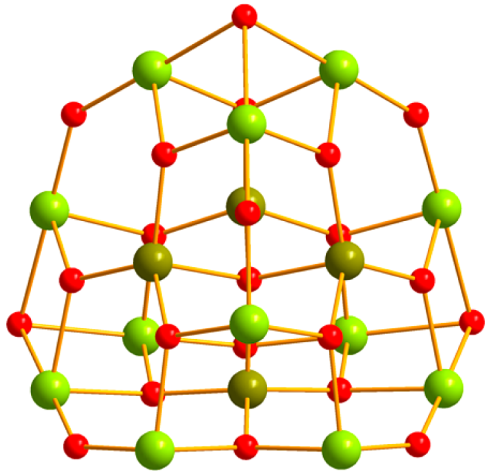

Figure 2. Polyhedral representation of the magnetic core of **1**. Color code: Fe (lime), disordered Fe (dark lime), O (red).

EXPERIMENTAL SECTION

General Methods and Materials. All reagents were used as purchased without further purification. The trilacunary POM precursors $Na_{12}[P_2W_{15}O_{56}]\cdot 24H_2O$, $K_{10}[A\text{-}\alpha\text{-}SiW_9O_{34}]\cdot 24H_2O$, and $Na_{10}[A\text{-}\alpha\text{-}GeW_9O_{34}]\cdot 25H_2O$ were prepared according to published procedures, and their respective purity was confirmed by infrared spectroscopy.[10]

Synthesis of $(CH_6N_3)Na_{30}[Fe_{14}O_6(OH)_{13}(P_2W_{15}O_{56})_4]\cdot 105H_2O\cdot 2NaCH_3COO$ (GuNa-1). $Fe(ClO_4)_3\cdot H_2O$ (0.22 g, 0.59 mmol) was dissolved in 20 mL of H_2O, and $Na_{12}[P_2W_{15}O_{56}]\cdot 24H_2O$ (0.88 g, 0.20 mmol) was added under stirring until a clear yellow solution was obtained. Solid CH_3COONa (2.00 g, 24.0 mmol) was then added to the solution in small portions, resulting in a final pH of around 6. The resulting mixture was stirred at 85 °C for 30 min, allowed to cool, and then filtered. This was followed by addition of 0.20 mL of 1 M guanidinium chloride, and slow evaporation at room temperature for a week led to the appearance of a brown, crystalline product, which was filtered off and air-dried. Yield: 240 mg (29% based on W). IR (2% KBr pellet, ν/cm^{-1}):

DOI: 10.1021/acs.inorgchem.5b00124
Inorg. Chem. 2015, 54, 6136−6146

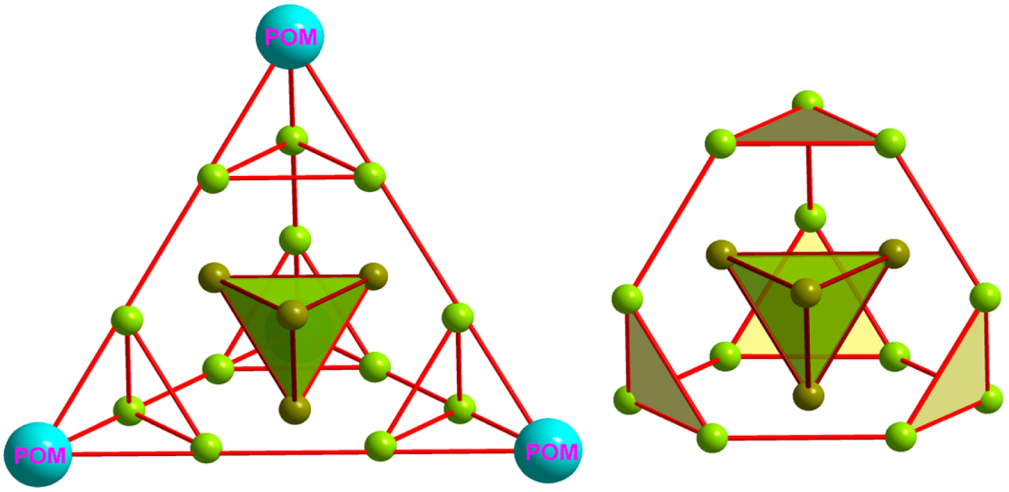

Figure 3. Combined polyhedral/ball-and-stick representation of **1** indicating the supertetrahedral geometry of **1**. Color code: Wells−Dawson POM unit (aqua), Fe (lime), disordered Fe (dark lime).

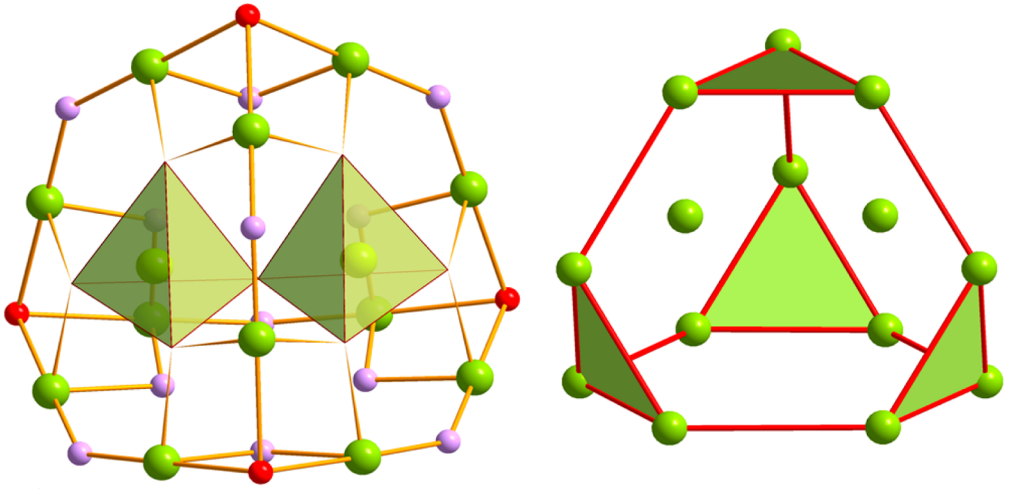

Figure 4. Combined polyhedral/ball-and-stick representation. Left shows magnetic core of **1**. Protonated oxygen atoms are shown in lavender. Right shows a truncated tetrahedron.

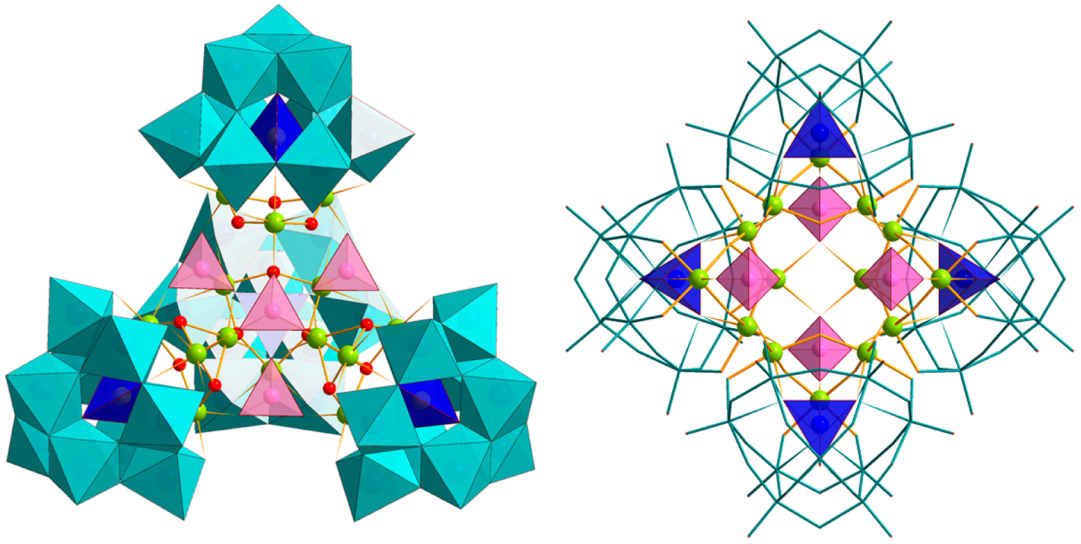

Figure 5. Combined polyhedral/ball-and-stick representation of **2** and **3**. Color code: WO_6 octahedra (aqua), Fe (lime), PO_4 (pink), XO_4 (blue), X = Ge, Si, O (red).

DOI: 10.1021/acs.inorgchem.5b00124
Inorg. Chem. 2015, 54, 6136−6146

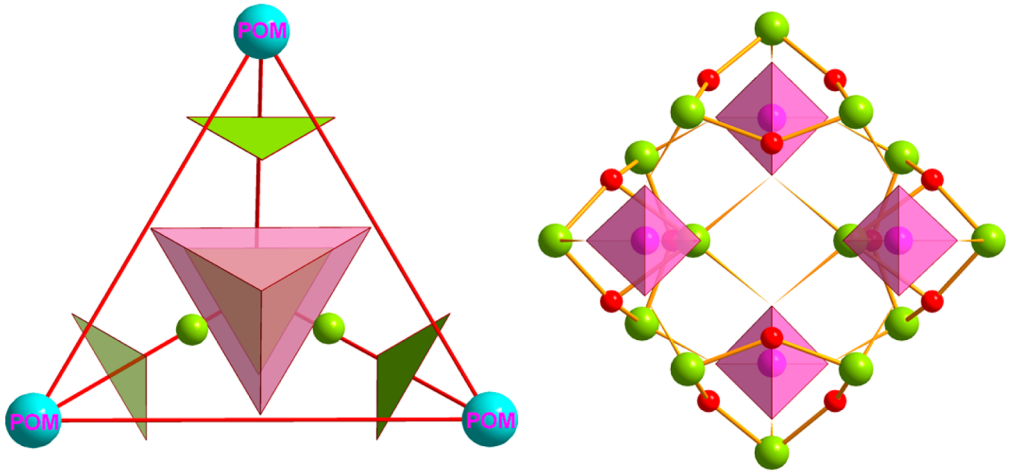

Figure 6. Combined polyhedral/ball-and-stick representation: (right) magnetic core of **2** and **3**, and (left) supertetrahedral geometry of **2** and **3**. Color code: Keggin POM unit (aqua), Fe (lime), PO_4 (pink), O (red).

1624(s), 1463(m), 1417(w), 1384(m), 1087(s), 943(s), 913(m), 728(s), 812(s), 724(s), 521(w), 459(w) (Figure S1 in the Supporting Information). Elemental analysis calculated (found): Na 3.81 (3.83), C 0.31 (0.35), H 1.51 (0.91), N 0.22 (0.19) Fe 4.05 (4.28), W 57.19 (57.56), P 1.28 (1.36).

Synthesis of $Cs_{4.5}K_{14}Na_{1.5}[Na_2Fe_{14}(OH)_{12}(PO_4)_4(A\text{-}\alpha\text{-}SiW_9O_{34})_4]\cdot 105H_2O\cdot 2Na_3PO_4$ (CsKNa-2). $FeCl_3\cdot 6H_2O$ (0.17 g, 0.63 mmol) was dissolved in 20 mL of H_2O, and $K_{10}[A\text{-}\alpha\text{-}SiW_9O_{34}]\cdot 24H_2O$ (0.52 g, 0.17 mmol) was added under stirring until a clear, dark yellow solution was obtained. Solid Na_3PO_4 (0.16 g, 0.9 mmol) was then added in small portions, and the turbid yellow-orange solution turned at pH ∼8.5 to a clear orange-brown solution; the final pH was around 9.0. This solution was stirred for 1 h at 70 °C. The resulting clear solution was left to cool down and filtered. After addition of 2−3 drops of 1 M CsCl, the solution was kept in an open vial at room temperature for slow evaporation. A dark orange-brown crystalline product started to appear which was collected after 2 weeks. Yield 105 mg (21% based on W). IR data (KBr pellet) in cm^{-1}: 1080(s), 991(w), 945(s), 791(s), 733(w), 526(w), 461(w) (Figure S2 in the Supporting Information). Elemental analysis (%), calculated (found): Na 1.60 (1.97), P 1.34 (1.13), Fe 5.69 (5.67), W 48.25 (48.90), Si 0.82 (0.89) Cs 4.35 (4.57), K 3.99 (4.05)

Synthesis of $Rb_4Na_{16}[Na_2Fe_{14}(OH)_{12}(PO_4)_4(A\text{-}\alpha\text{-}GeW_9O_{34})_4]\cdot 139H_2O\cdot 2Na_3PO_4$ (RbNa-3). $FeSO_4\cdot 7H_2O$ (0.28 g, 1.00 mmol) was dissolved in 20 mL of H_2O, and $Na_{10}[A\text{-}\alpha\text{-}GeW_9O_{34}]\cdot 25H_2O$ (0.50 g, 0.17 mmol) was added. The resulting solution turned to a dark green color. Addition of 0.5 g of Na_3PO_4 in small portions followed, while the pH was adjusted to be around 8.0 with 1 M HCl. The resulting turbid dark green solution was stirred at 70−75 °C for an hour and was then cooled down and decanted by centrifugation. Three to four drops of 1 M RbCl were added to the obtained clear solution which was kept in an open vial for slow evaporation. The color of solution turned orange in 3 weeks, and an orange crystalline product was collected after 4 weeks. Yield 120 mg (24% based on W). IR data (KBr pellet) in cm^{-1}: 1087(s), 943(s), 876(m), 802(s), 721(w), 526(w), 466(w) (Figure S2 in the Supporting Information). Elemental analysis (%), calculated (found): Na 3.93 (4.20), P 1.32 (1.31), Fe 5.55 (5.46), W 47.14 (46.30), Ge 2.06 (2.40) Rb 2.43 (2.52).

IR, TGA, and Elemental Analysis Measurements. Infrared spectra were recorded on a Nicolet Avatar 370 FT-IR spectrophotometer using KBr pellets. The following abbreviations were used to assign the peak intensities: w = weak, m = medium, and s = strong. Thermogravimetric analyses were carried out on a TA Instruments SDT Q600 thermobalance with a 100 mL/min flow of nitrogen; the temperature was ramped from 20 to 800 °C at a rate of 5 °C/min. Elemental analyses were performed by CNRS, Service Central d'Analyze, Solaize, France.

X-ray Crystallography. Each crystal was mounted on a Hampton cryoloop in light oil for data collection at 100 K. Indexing and data collection were performed on a Bruker D8 SMART APEX II CCD diffractometer with κ geometry and Mo Kα radiation (graphite monochromator, λ = 0.710 73 Å). Data integration was performed using SAINT.[11] Routine Lorentz and polarization corrections were applied. Multiscan absorption corrections were performed using SADABS.[12] Direct methods (SHELXS) successfully located the tungsten atoms, and successive Fourier syntheses (SHELXL) revealed the remaining atoms.[13] Refinements were full-matrix least-squares against $|F^2|$ using all data. In the final refinement, all nondisordered heavy atoms (P, Ge, Si, W, Fe, Rb, Cs, Na, K) were refined anisotropically, whereas oxygen atoms and disordered countercations were refined isotropically. Crystallographic data are summarized in Table 1.

Magnetic Susceptibility Measurements. The magnetic susceptibility measurements were obtained with the use of a Quantum Design SQUID magnetometer MPMS-XL. This magnetometer works between 1.8 and 400 K for dc applied fields ranging from −7 to 7 T. Measurements were performed on polycrystalline samples. The magnetic data were corrected for the sample holder and the diamagnetic contribution.

Electrochemical Experiments. Pure water was obtained with a Milli-Q Intregral 5 purification set. All reagents were of high-purity grade and were used as purchased without further purification: H_2SO_4 (Sigma-Aldrich), H_3PO_4 (Sigma-Aldrich), anhydrous Na_2SO_4 (Riedel-de Haën), $LiCH_3COO\cdot 2H_2O$ (Fluka), and CH_3COOH (Carlo Erba). The composition of the various media was as follows: for pH 2.0 and 3.0, 0.5 M Li_2SO_4 + H_2SO_4; for pH 5.0 and 6.0, 1.0 M $LiCH_3COO$ + CH_3COOH.

The stability of these polyanions in solution as a function of the pH and time was studied by monitoring the evolution of their UV−vis spectra at least over 24 h. Such duration is long enough for the electrochemical characterization of the compound and its possible application in electrocatalysis processes. Compound **1** was found to be stable in media having pH values ranging from 2 and up to at least 6. Compounds **2** and **3** slowly decay with the concomitant dissociation of Fe^{III} ions. Nevertheless, we were able to characterize them by cyclic voltammetry upon recording the CVs just after their solubilization. This is presented in the Supporting Information (Figures S16 and S17).

The UV−vis spectra were recorded on a PerkinElmer 750 spectrophotometer with 0.8 mM solutions of the polyanion. Matched 2.00 mm optical path quartz cuvettes were used.

Electrochemical data were obtained using an EG&G 273 A potentiostat driven by a PC with the M270 software. A one-compartment cell with a standard three-electrode configuration was used for cyclic voltammetry experiments. The reference electrode was a saturated calomel electrode (SCE) with the counter electrode platinum gauze having a surface area larger than that of the working electrode; both electrodes were separated from the bulk electrolyte solution via fritted compartments filled with the same electrolyte. The working electrode was a glassy carbon stick (GC, Le Carbone-Lorraine, France) whose immersed tip had the dimensions of ca. 15 × 8 × 1.5 mm^3. The pretreatment of this electrode before each experiment was adapted from a method described elsewhere.[14] The stick was polished twice with SiC paper, grit 500 (Struers). After each polishing step, which took about

DOI: 10.1021/acs.inorgchem.5b00124
Inorg. Chem. 2015, 54, 6136−6146

Table 1. Crystal Data for GuNa-1, CsKNa-2, and RbNa-3

	GuNa-1	CsKNa-2	RbNa-3
empirical formula	$C_5H_{235}Fe_{14}N_3Na_{32}O_{352}P_8W_{60}$	$Cs_{4.50}H_{222}Fe_{14}K_{14}Na_{9.50}O_{277}P_6Si_4W_{36}$	$Fe_{14}Ge_4H_{290}Na_{24}O_{311}P_6Rb_4W_{36}$
fw, g/mol	18767.3	13718.4	14 038.7
cryst syst	trigonal	orthorhombic	orthorhombic
space group	$R\bar{3}$	*Pmmn*	*Pmmn*
a, Å	29.784(3)	22.7572(10)	22.690(2)
b, Å	29.784(3)	27.8330(12)	27.943(3)
c, Å	76.121(12)	18.7848(8)	18.793(2)
α, deg	90	90	90
β, deg	90	90	90
γ, deg	120	90	90
V, Å^3	58479(16)	11898.3(9)	11915(2)
Z	6	2	2
D_{calcd}, g/cm^3	3.197	3.829	3.875
abs coeff	18.299	19.289	19.660
cryst size, mm^3	0.40 × 0.40 × 0.10	0.29 × 0.28 × 0.18	0.24 × 0.17 × 0.05
θ range, deg	3.396−23.252	3.43-21.43	3.42−26.37
reflns collected	320 095	91 087	338 779
indep reflns	18 619	7134	9936
R(int)	0.1508	0.0928	0.0908
obsd ($I > 2\sigma(I)$)	11 954	5879	9015
GOF on F^2	1.002	1.119	1.072
R1 $[I > 2\sigma(I)]^a$	0.0832	0.0536	0.0660
wR2 (all data)^b	0.1421	0.1295	0.1628

$^a R = \sum||F_o| - |F_c||/\sum|F_o|$. $^b R_w = [\sum w(F_o^2 - F_c^2)^2/\sum w(F_o^2)^2]^{1/2}$.

5 min, the stick was rinsed and sonicated twice in Millipore water for 5 min. Prior to each experiment, solutions were thoroughly deaerated for at least 30 min with pure Ar. A positive pressure of this gas was maintained during subsequent work. All cyclic voltammograms were recorded at a scan rate of 10 mV s^{-1}, and potentials are quoted against the saturated calomel electrode (SCE) unless otherwise stated. The polyanion concentration was 0.8 mM. All experiments were performed at room temperature, which is controlled and fixed for the laboratory at 20 °C. Results were reproducible, and slight variations were observed over successive runs due to the uncertainty associated with the detection limit of our equipment (potentiostat, hardware, and software) and not due to the working electrode pretreatment nor to possible fluctuations in temperature.

RESULTS AND DISCUSSION

Synthesis and Structure. The 14-iron(III)-containing 60-tungsto-8-phosphate(V) $[Fe_{14}O_6(OH)_{13}(P_2W_{15}O_{56})_4]^{31-}$ (**1**) was synthesized in a one-pot reaction of the trilacunary polyanion precursor $[P_2W_{15}O_{56}]^{12-}$ with Fe^{III} in slightly acidic, aqueous solution in the presence of acetate ion. Polyanion **1** crystallizes as the hydrated, mixed guanidinium-sodium salt $(CH_6N_3)Na_{30}[Fe_{14}O_6(OH)_{13}(P_2W_{15}O_{56})_4]\cdot 105H_2O$ (**GuNa-1**) in the trigonal space group $R\bar{3}$. Single-crystal X-ray diffraction analysis reveals that **1** consists of a cationic $\{Fe_{14}O_6(OH)_{13}\}^{17+}$ core stabilized by four trilacunary $[P_2W_{15}O_{56}]^{12-}$ Wells−Dawson units in a tetrahedral fashion (Figure 1). The three iron ions in each $\{Fe_3P_2W_{15}\}$ unit occupy the octahedral sites of an edge-shared triad in the parent $[P_2W_{18}O_{62}]^{6-}$ structure. The four tri-Fe^{III}-substituted Wells−Dawson units $\{Fe_3P_2W_{15}\}$ are linked via protonated Fe−(OH)−Fe bonds, resulting in overall T_d symmetry (Figure 1). In the central cavity of the assembly, four equivalent and tetrahedrally coordinated positions can be found, which are 50% occupied by two extra Fe^{III} ions (Figures 2 and 3), resulting in two central, corner-shared $\{FeO_4\}$ tetrahedra. This disorder breaks the overall symmetry of the polyanion to C_{2v}. The outer 12 Fe^{III} ions in **1** are hexacoordinated in idealized octahedral fashion with Fe−O bond lengths in the range 1.87(3)−2.27(2) Å, whereas the two encapsulated iron centers exhibit substantial deviation from a regular tetrahedron, with the largest deviation being seen for the bond angle O24F−Fe2−O12F (99.7(11)°), with bond lengths in the range 1.86(2)−2.00(2) Å. However, these bond lengths and angles are not completely reliable due to disorder of the inner iron(III) centers. According to bond valence sum (BVS) calculations,[15a−c] all the μ_2-oxo ligands in the $\{Fe_{14}O_6(OH)_{13}\}^{17+}$ assembly are monoprotonated with BVS values ranging from 1.03 to 1.45, while all the μ_3-oxo ones are nonprotonated (Figure 4, left). Concerning the iron centers, BVS showed that the two inner, tetrahedrally coordinated centers had a lower valency (2.57−2.68) compared to those of the outer, octahedrally coordinated ones (3.02−3.09). These relatively low values are most probably due to the crystallographic disorder of these centers; this effect has been previously seen in other, related compounds.[6l,15d] As such, the iron assembly in **1** can be attributed to a $[Fe_{14}O_6(OH)_{13}]^{17+}$ core stabilized by four $[P_2W_{15}O_{56}]^{12-}$ lacunary units, leading to a total charge of 31−, which is balanced by 30 sodium and one guanidinium countercations in the solid state. The numbers of countercations and water molecules were determined by elemental and thermogravimetric (TGA) analyses (see Experimental Section and Supporting Information Figure S3). Polyanion **1** is structurally closely related to the recently published polyanion $[Fe_{13}P_8W_{60}O_{227}(OH)_{15}(H_2O)_2]^{30-}$ (Fe_{13}) by Cronin and co-workers, which consists of the same four encapsulating tri-iron(III)-substituted Wells−Dawson units; however, in this case only one extra Fe(III) center is present which is disordered over four positions.[6l] The coordination geometry of the central Fe^{III} in Fe_{13} is trigonal-bipyramidal, in contrast to the two corner-shared $\{FeO_4\}$ tetrahedral units in **1**. Tetrahedrally coordinated iron(III) centers in POM structures are present as heteroatoms in compounds such as $[(Fe_4W_9O_{34}(H_2O))_2(FeW_6O_{26})]^{19-}$ and $[Fe_4(H_2O)_2(FeW_9O_{34})_2]^{10-}$.[5f] With regard to the synthetic procedure, slow addition of sodium acetate after dissolution of the reactants

DOI: 10.1021/acs.inorgchem.5b00124
Inorg. Chem. 2015, 54, 6136−6146

plays a crucial role for the formation of polyanion **1**. Attempts to isolate **1** in acetate buffer solutions of different concentrations, or by adding sodium formate instead, were not successful.

Reaction of $FeCl_3 \cdot 6H_2O$ with $K_{10}[A\text{-}\alpha\text{-}SiW_9O_{34}] \cdot 24H_2O$, and $FeSO_4 \cdot 7H_2O$ with $Na_{10}[A\text{-}\alpha\text{-}GeW_9O_{34}] \cdot 25H_2O$, in ratios of 3:1 and 6:1, respectively, in sodium phosphate buffer (pH 8−8.5) at 70 °C resulted in the formation of the two tetrameric, 14-Fe^{III}-containing tungstosilicate $[Na_2Fe^{III}_{14}(OH)_{12}(PO_4)_4(A\text{-}\alpha\text{-}SiW_9O_{34})_4]^{20-}$ (**2**) and tungstogermanate $[Na_2Fe^{III}_{14}(OH)_{12}(PO_4)_4(A\text{-}\alpha\text{-}GeW_9O_{34})_4]^{20-}$ (**3**). Polyanions **2** and **3** are isostructural and crystallize in the orthorhombic space group *Pmmn*; therefore, only the structure of **2** is discussed here in detail.

Single-crystal X-ray analysis revealed that the tetrameric polyanion **2** is composed of four tri-Fe^{III}-substituted *A*-α-Keggin units, $[Fe_3(OH)_3SiW_9O_{34}]^{4-}$, connected by four phosphate linkers in a tetrameric fashion with idealized T_d point group symmetry (Figure 5). In a similar fashion to that of **1**, four equivalent, octahedrally (as opposed to tetrahedrally in **1**) coordinated positions are found in the central cubane cavity of the Keggin assembly, (Figure 6). These positions are also occupied by two Fe^{III} centers, each with a 50% crystallographic occupancy, breaking the symmetry of polyanion **2** to C_{2v}. The Fe−O bonds in the central M_4O_4 cubane unit are relatively long for two disordered Fe^{III} centers (ca. 2.2−2.3 Å), leading to low BVS values (*vide infra*). Careful evaluation of various disorder models revealed that the four positions are further occupied by two sodium ions with 50% occupancy (see Supporting Information Figure S4). Such arrangement leads to a neutral $\{Na_2Fe^{III}_2O_4\}$ assembly, fully consistent with the $\{Co^{II}_4O_4\}$ unit in our related Co_{16}−POM analogues.[7e,g] All fully occupied Fe^{III} centers are hexacoordinated with distorted octahedral geometry, and the Fe−O bond lengths are in the range 1.90(2)−2.22(1) Å. Protonated oxygens of the polyanion were located by bond valence sum (BVS) calculations, which indicated that the μ_3-O bridges linking the three iron ions in the trisubstituted Keggin units are monoprotonated with BVS values 1.27−1.36. The BVS values for the iron centers in the $[Fe_3(OH)_3SiW_9O_{34}]^{4-}$ units range from 2.84 to 3.02, and those for the inner two disordered ones range from 1.28 to 1.55, respectively. As mentioned above, these low BVS values are due to the central M_4O_4 cubane unit being formed by two disordered Fe^{III} and Na^+ ions. The total charge of **2** is therefore 20−, which is balanced in the solid state by 1.5 sodium, 14 potassium, and 4.5 cesium countercations. For polyanion **3**, the charge is balanced in the solid state by 16 sodium and four rubidium countercations. The countercations and crystal waters for both polyanion salts were determined by elemental and thermogravimetrical analysis (see Experimental Section and Supporting Information Figure S5).

Recently, our group has reported the family $\{Co_{16}(XW_9)_4\}$, which are structural Co^{II} analogues of **2** and **3**, comprising $\{Co_4O_4\}$ cubane cores with no disorder, leading to a complete $\{Co_{16}\}$ aggregate stabilized by four $\{XW_9O_{34}\}$ (X = P^V, Si^{IV}, Ge^{IV}) Keggin units.[7e,g] Some Keggin-type polyanions with a 13-iron(III)-oxo core have been reported, such as $[\{(Fe^{III}_3Fe^{II}_{0.25}(OH)_3)(AsO_4)(B\text{-}\alpha\text{-}AsW_9O_{34})\}_4]^{22-}$, $[\{(B\text{-}\alpha\text{-}PW_9O_{34})Fe_3(OH)_3\}_4(PO_4)_4Fe]^{22-}$, and $[\{Fe^{II}_{1.5}Fe^{III}_{12}(\mu_3\text{-}OH)_{12}(\mu_4\text{-}PO_4)_4\}(B\text{-}\alpha\text{-}PW_9O_{34})_4]^{18-}$.[6g,j,k] These reported structures are all based on *B*-α-type trilacunary POM ligands, whereas **2** and **3** are based on *A*-α-type ligands.

Several details in the synthetic conditions need to be considered for the successful isolation of polyanions **2** and **3**. For instance, compound **2** is obtained only by using the potassium salt of $[A\text{-}\alpha\text{-}SiW_9O_{34}]^{10-}$, rather than for example the sodium salt, indicating once again the importance of countercations during POM synthethis.[10c] Furthermore, the synthesis of **3** is only possible using an iron(II) salt (e.g., $FeSO_4 \cdot 7H_2O$) instead of iron(III). Apparently the iron centers in **3** are all oxidized from Fe^{II} to Fe^{III} by air oxygen during the reaction and crystallization period (the compound is left to crystallize in an open container). Also, in a comparison with **2**, polyanion **3** requires a larger Fe^{II} to POM precursor ratio (6:1) and a larger amount of added Na_3PO_4 in order to drive the formation of a pure, crystalline product.

Topological Features. In recent years, a methodology[16] has been established to facilitate the classification, enumeration, and description of the topology of high polynuclear coordination clusters,[17,18] where each metal center is considered as a node and every monatomic bridge (O, N, S) is taken as a linker. This approach can also be very easily applied in polyoxometalate chemistry.[7g]

In the present study, all three polyanions **1-3** contain four Fe sites in the center of the cluster with 50% occupancy, and thus, the ideal approach to describe their topology is 2-fold, either considering full or vacant occupancy for those 4 Fe ions. With the consideration of full occupancy of the four central ions and the exclusion of all counteranions from the simplification process, polyanion **1** can be described as a skeleton enumerated as **4,4,4,7,9M76-1** (Figure 7, upper left) while the central Fe unit can be described as a hexadecanuclear **5,9M16-1** motif (Figure 7, upper right). A search in the Polynuclear Inorganic Clusters Database[16] shows the following: (a) this topology has never been found in any metal, (b) only 6 other Fe_{16} examples (LULMEK, QADLIR, RAPWUA, RAPXAH, TIQDAZ, UVITUP) exist, and (c) the motif of all the previous reported Fe_{16} examples is not related to that of polyanion **1**. More interestingly, with this approach, it is also possible to perform a graph search and thus easily obtain a correlation of the Fe_{16} core. In this context, the **5,9M16-1** motif can be found as a part of the supertetrahedron (*T*3) **3,6,9M20-1** found in Mn_{20}[19] (Supporting Information Figure S6), and thus the Fe_{16} core can be considered as a defective supertetrahedron (*T*3) missing the four corners. By excluding the central four Fe ions and counteranions from the simplification process, polyanion **1** can be numerically represented as **4,4,4,5M72-1** (Supporting Information Figure S7, left) while the central Fe_{12} core possess a **3M12-1** (Supporting Information Figure S7, right) topology which according to a literature survey[16] has been seen only in Co and Ni chemistry (CITWIM, DAJYUK, DAJZAR, DAJZEV, KELKIX). In a similar manner, the simplification process for compounds **2** and **3**, considering full Fe occupancies for the four inner metal sites and not considering the two Na ions, indicates that **2** and **3** are isoskeletal and results in both cases in **4,4,5,6M52-1** (Figure 7, lower left) and **3,6M16-1** (Figure 7, lower right) skeletons for the whole structure and the Fe cluster, respectively. The latter skeletons could be identified in the recently reported Co_{16} polyanion.[7g] Simplifying the structures of **2** and **3**, excluding the inner four metal sites, results in a **4(4M12−1)** motif (Supporting Information Figure S7).

Magnetic Measurements. Direct current susceptibility measurements on the salts of polyanions **1**−**3** were performed in the temperature range 1.8−300 K under a field of 1000 Oe. Plots of χT product versus temperature for the different salts of **1**−**3** are shown in Figure 8. On lowering the temperature, the χT values of all the compounds decrease steadily. This type of behavior indicates the presence of dominant antiferromagnetic interactions in **1**−**3**. The χT product of **1**−**3** continuously decreases from 33.43, 26.90, and 31.05 cm^3 K/mol per molecule at 300 K to 2.95, 3.10, and 6.61 cm^3 K/mol per polyanion, respectively, at 1.8 K. This result demonstrates that the metal centers

DOI: 10.1021/acs.inorgchem.5b00124
Inorg. Chem. 2015, 54, 6136−6146

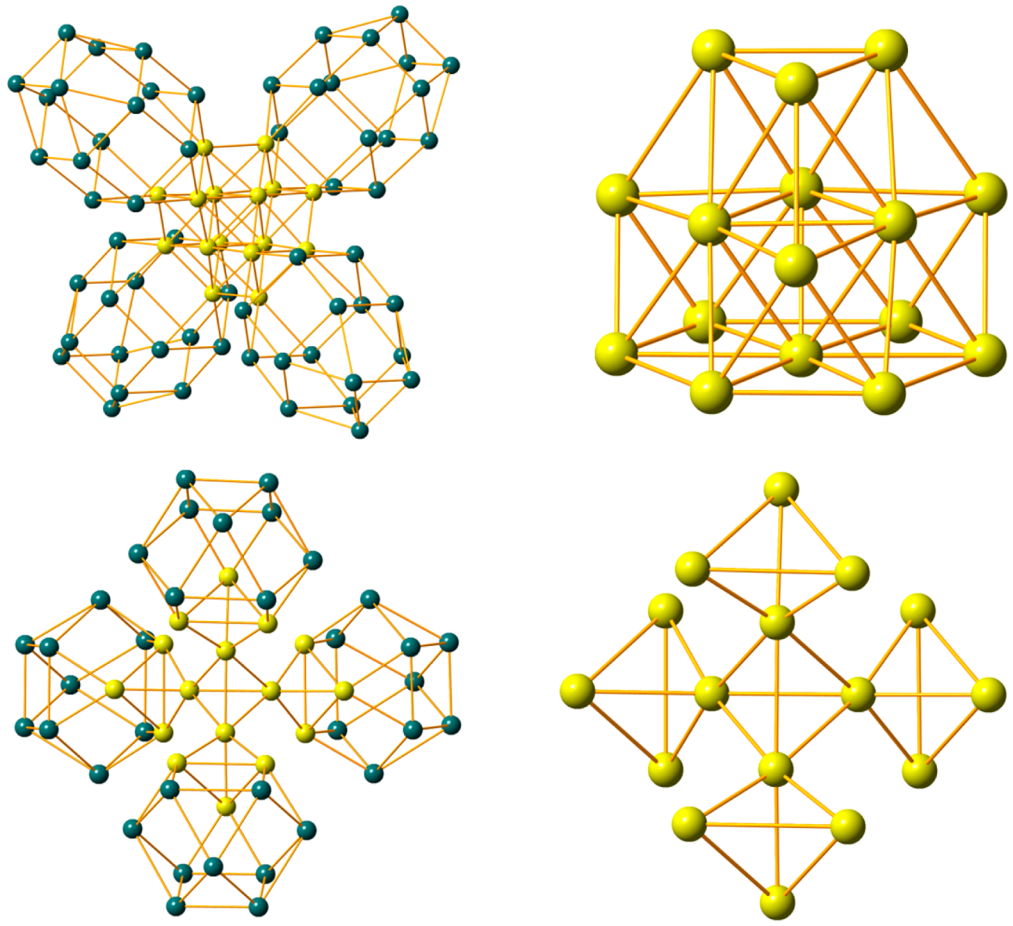

Figure 7. (Upper) Decorated motifs for polyanion **1**, **4,4,4,7,9M76-1** (left), and **5,9M16-1** (right) considering full occupancy for the inner 4 Fe ions. (Lower) Decorated motifs for polyanions **2** and **3**, **4,4,5,6M52-1** (left) and **3,6M16-1** (right), considering full occupancy for the inner 4 Fe ions. Color code: W (turquoise balls), Fe (lime balls).

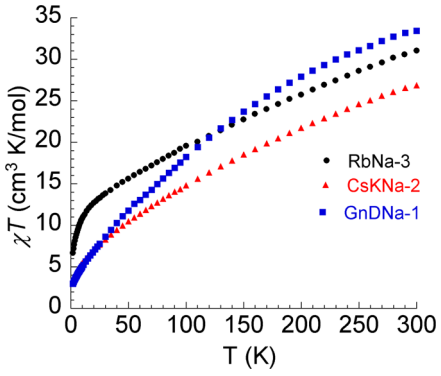

Figure 8. Plot of χT vs T under applied dc field of 0.1 T for the salts of **1**−**3**.

are coupled antiferromagnetically. The χT values at 300 K for **1**−**3** are well below the theoretically expected value of 14 noninteracting $S = {}^{5}/_{2}$ spins (61.26 cm^3 mol^{-1} K), indicating large antiferromagnetic interactions.[6c,f,j] The polyanions **1**−**3** are even electron systems, and the theoretical minimum spin state is $S = 0$, when 70 electrons are spin-paired. An effort to estimate the total ground spin state was made on the basis of an extrapolation of the χT to 0 K from the lowest temperature section of the χT versus temperature curve. The extrapolated value of χT at 0 K is ~2.5 cm^3 K/mol for **1** and **2**, and ~5.0 cm^3 K/mol for **3**. The fact that these values are nonzero, and much smaller than the value 8.74 cm^3 K/mol calculated for two iron(III) ions with a total spin of $S = 5$ and $g = 2.00$, indicates that some of the iron centers within the polyanions are not precisely antiparallel, but slightly canted to produce a weak ferromagnetic moment. Another observation is that the χT curves for these compounds do not reach saturation, even at room temperature, demonstrating the presence of a high density of electronic states that are thermally accessible.

The lack of saturation for the χT versus T curves is also reflected in the absence of saturation in the magnetization versus magnetic field (Supporting Information Figures S8−S10). The magnetization keeps increasing without saturation as the field increases. The maximum values at 2 K were 6.57, 7.01, and 13.95 μ_B, respectively, for **1**−**3**. These values are too large to be expected only from the population of the low-lying excited states with increasing external magnetic field. Therefore, we believe that this behavior is mostly due to a field-induced transition from very weakly antiferromagnetic to an almost parallel and weakly ferromagnetic arrangement[20] for some of the Fe magnetic moments, a conclusion which also supports the observation from the low-temperature χT curve. This is not unusual and unexpected given the wide range of Fe−O−Fe angles and protonation of bridging oxo ligands in polyanions **1**−**3**.

Electrochemistry. As previously stated, only polyanion **1** is sufficiently stable in solution to be thoroughly studied by electrochemistry and possibly used in electrocatalytic applications. In order to elucidate the electrochemical features of **1**, we have

DOI: 10.1021/acs.inorgchem.5b00124
Inorg. Chem. 2015, 54, 6136−6146

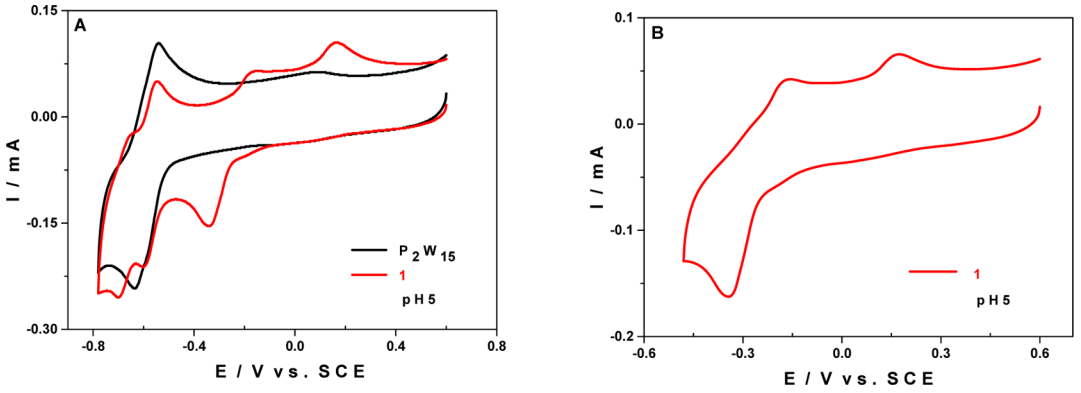

Figure 9. Cyclic voltammograms of $[P_2W_{15}O_{56}]^{12-}$ (0.32 mM) and **1** (0.08 mM) in a 1.0 M $LiCH_3COO$ + CH_3COOH/pH 5 buffer solution. The scan rate was 10 mV s^{-1}. The working electrode was glassy carbon, and the reference electrode was SCE. For more detailed information, see the Experimental Section. (A) Superposition of $[P_2W_{15}O_{56}]^{12-}$ (black) and **1** (red). (B) Cyclic voltammogram of **1** with the reduction potential domain restricted to the Fe^{III} centers.

compared the behavior of this polyanion to that of its lacunary precursor $[P_2W_{15}O_{56}]^{12-}$ in 1.0 M $LiCH_3COO$ + CH_3COOH/pH 5 buffer, a medium in which the two species are sufficiently stable in the time scale of a cyclic voltammetry experiment. Their concentrations have been adjusted in order to render the peak potential comparison more clear. At pH 5, the CV of $[P_2W_{15}O_{56}]^{12-}$ exhibits two successive redox waves due to the reduction of the W^{VI} centers, the first one involving 4 electrons and the second 2 electrons.[22] In the CV shown in Figure 9A, the potential range has been restricted, on the negative side, to the first reversible wave (−0.78 V vs SCE).

When the CV of **1** is compared to that of $[P_2W_{15}O_{56}]^{12-}$ taken as a reference, two important differences are noticed: (1) There is a new reduction wave peaking at potential values less negative than those for the W^{VI} centers. This wave is attributed to the reduction of Fe^{III} centers, which are known to be more easily reduced than the W^{VI} centers.[6b,21] (2) There is splitting of the reduction wave of the W^{VI} centers, which changes from a single reversible step (E_{pc} = −0.63 V vs SCE) into a sequence of two reversible steps (E_{pc1} = −0.60 V and E_{pc2} = −0.70 V vs SCE). As far as the Fe^{III} centers included in **1** are concerned, it seems that their reduction takes place in a single step (E_{pc} = −0.34 V vs SCE), a result which has been observed for the majority of POMs containing at least 6 Fe^{III} centers.[3h,6c,d,f] This outcome suggests that the 14 Fe^{III} centers, even if they are not all equivalent, seem to be simultaneously reduced (Supporting Information Figure S11). Interestingly, their reoxidation takes place in two steps. The first one looks quasireversible with respect to the previous reduction and peaks at −0.16 V versus SCE. It is followed by a second wave located at far more positive potentials values (E_{pa} = +0.16 V vs SCE) which is totally irreversible with respect to the previous reduction. If we recall the studies on the release of Fe^{III} centers upon reduction for several POMs,[22] this second wave may be easily attributed to the oxidation of noncoordinated Fe^{II} centers. This phenomenon has been studied in a less acidic medium (pH 6) which released Fe^{III} ions forming hydroxides and oxides whose subsequent reduction may be observed (Supporting Information Figure S14).

Controlled potential coulometry (CPC) carried out at a constant potential of −0.48 V versus SCE revealed a consumption of 14.5 ± 0.1 electrons per polyanion **1**, which were almost totally recovered upon reoxidation at a potential of +0.60 V versus SCE (13.8 ± 0.1 electrons per polyanion see Supporting Information Figure S11). The comparison of the CVs of **1** before reduction and after total reoxidation of the Fe centers (Supporting Information Figure S12) shows that the redox peak potentials of the latter markedly changed, whereas the responses due to the W centers were not affected. The reduction of the Fe centers takes place now in three consecutive steps, at far more positive potentials (E_{pc1} = +0.02 V, E_{pc2} = −0.12 V and E_{pc3} = −0.23 V vs SCE), but the total number of electrons involved remains close to 14. This indicates that there has been a reorganization of the Fe^{III} centers within the Fe_{14} cluster with respect to the four $[P_2W_{15}O_{56}]^{12-}$ fragments, without any Fe loss. This is consistent with the results obtained by UV−vis spectrophotometry with samples tested before reduction, after reduction, and after reoxidation of all the Fe^{III} centers (Supporting Information Figure S13).

As mentioned above, the exchange of such a large number of electrons per polyanion containing several Fe^{III} centers was observed before and led to the development of electrocatalytic applications.[3h,6c,d,f] In the present study, we have decided to work in low pH media (pH 2 and 3) in order to avoid the formation of Fe hydroxides and oxides which may interfere at higher pH (Supporting Information Figure S14). When the experiments were carried out in media having lower pH values, the main redox waves of **1** shifted toward less negative potentials, as expected. At pH 3, the reduction of the 14 Fe^{III} centers still occurs in a single step (E_{pc} = −0.10 V vs SCE), whereas, at pH 2, three distinct waves are observed (Figure 10A). A slow scan rate scan (2 mV s^{-1}) allowed the identification of a first reversible step (E_{pc1} = +0.35 V; E_{pa1} = +0.44 V) followed by two equally reversible steps (E_{pc2} = +0.15 V; E_{pa2} = +0.25 V and E_{pc3} = +0.02 V; E_{pa3} = +0.09 V; Figure 10B). To the best of our knowledge, this is the first example of a polyanion containing Fe^{III} centers which are reversibly reduced at such positive potentials.

This feature led us to study the electrocatalytic properties of **1** with respect to several substrates in the 0.5 M Li_2SO_4 + H_2SO_4/pH 2 medium where the compound is stable and the waves associated with the reduction of the Fe^{III} centers exhibit a reversible behavior.

Electrocatalytic Reduction of Dioxygen and Hydrogen Peroxide. Dioxygen was selected as the first candidate in the present work because it is abundant and environmentally benign, yet very challenging to use as a selective oxidant.[23] Hydrogen peroxide was also selected as a substrate because it may be useful in assessing the nature of the final product in the electrocatalytic reduction of dioxygen. It is also an important oxidant in its own right.

In this medium, the direct reduction of dioxygen on a glassy carbon electrode takes place at far more negative potentials

DOI: 10.1021/acs.inorgchem.5b00124
Inorg. Chem. 2015, 54, 6136−6146

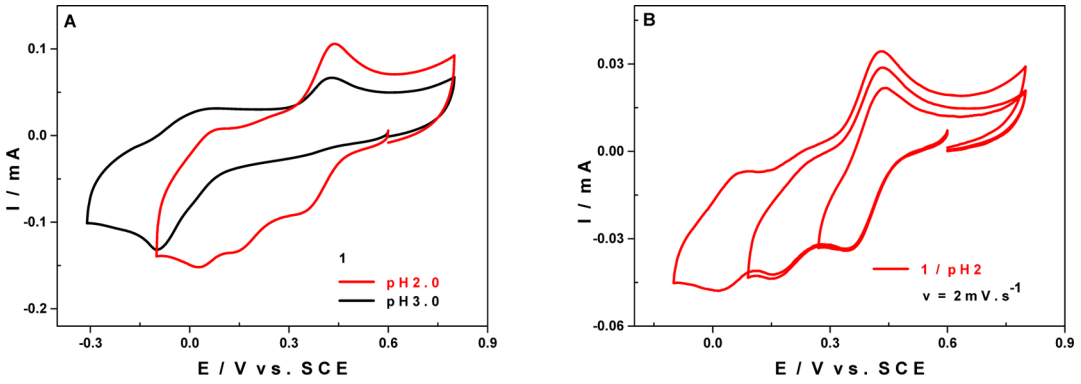

Figure 10. (A) Cyclic voltammograms of **1** in 0.5 M Li_2SO_4 + H_2SO_4/pH 2 (red) and pH 3 (black), the potential scan being restricted to the waves associated with the Fe^{III} centers at a scan rate of 10 mV s^{-1}. (B) Cyclic voltammograms obtained at a scan rate of 2 mV s^{-1}, with the reverse potentials at E_c = +0.27, +0.09, and −0.10 V vs SCE, respectively.

(Supporting Information Figure S15). In the presence of **1**, the reduction of O_2 starts at the second reduction wave involving Fe^{III} centers, with the onset potential being around +0.16 V versus SCE. At this potential, several Fe^{III} centers have already been reduced to the +2 oxidation state.[24] This hints at the formation of iron-oxo complexes as intermediates in the reduction of O_2 to H_2O, concomitant with the regeneration of the catalyst **1**.[25] In fact, in Figure 11 we observe that the

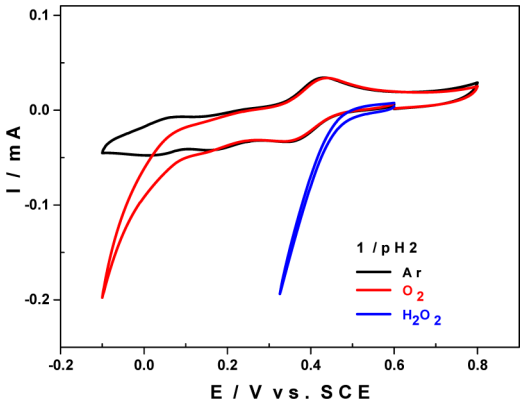

Figure 11. Cyclic voltammograms of **1** in 0.5 M Li_2SO_4 + H_2SO_4/pH 2, alone in an argon atmosphere (black), in the presence of dioxygen (red) and in the presence of hydrogen peroxide (blue). The scan rate was 2 mV s^{-1}, the working electrode was glassy carbon, and the reference electrode was SCE.

electrocatalytic reduction of H_2O_2 is effective for potential values around +0.50 V versus SCE (blue CV), which shows that **1** reduces H_2O_2 more easily than O_2, and confirms that the final product for the electro-reduction of O_2 by **1** is H_2O.

Reduction of Nitrogen Oxides, NO_3^- and NO. The most effective POMs for the electrocatalytic reduction of nitrate ions are those containing Cu^{II} or Ni^{II} centers.[26] To the best of our knowledge, just two heteropolytungstates containing Fe^{III} centers have been shown to possess a catalytic activity toward the reduction of nitrate ions: the species $[Fe_6(OH)_3(A\text{-}\alpha\text{-}GeW_9O_{34}(OH)_3)_2]$[11,6c] and $[P_8W_{48}O_{184}Fe_{16}(OH)_{28}(H_2O)_4]$.[20,6f] In both cases, the accumulation of Fe^{III} centers seems to play a crucial role, since they bring about a sufficiently large number of electrons so that the whole process may reach completion. As in the case of the electrocatalytic reduction of dioxygen described above, experiments were carried out in the same medium, 0.5 M Li_2SO_4 + H_2SO_4/pH 2. Figure 12 shows that **1** is efficient for the

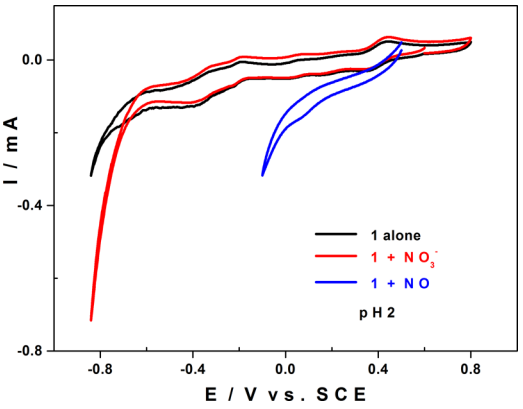

Figure 12. Cyclic voltammograms of **1** in 0.5 M Li_2SO_4 + H_2SO_4/pH 2, alone in an argon atmosphere (black), in the presence of nitrate ions (red) and in the presence of nitrogen monoxide (blue). The scan rate was 2 mV s^{-1}, the working electrode was glassy carbon and the reference electrode was SCE.

electrocatalytic reduction of nitrate ions. This process takes place after the reduction of the W centers of the polyanion. Its catalytic efficiency may be calculated by CAT = 100 × $\{[I(POM + NO_3^-) - I(POM)]/I(POM)\}$,[27] where $I(POM)$ and $I(POM + NO_3^-)$ are the POM reduction currents in the absence and in the presence of nitrate ions, yielding a value of 125%. A question arises concerning the extent of the reduction: How much is the oxidation number of nitrogen modified? After the pioneering works on the reduction of nitrite ions by POMs both by Anson et al.[28] and by Nadjo et al.,[29] this reaction is used as a classic test to assess the catalytic properties of POMs. In our experimental conditions, at pH 2, nitrite ions, NO_2^-, exist rather in the form of nitrous acid, HNO_2, and nitric oxide, NO. In fact, the pK_a for the reaction given by the equation $HNO_2 = H^+ + NO_2^-$ is 3.3, and HNO_2 disproportionates according to the following equation: $3HNO_2 = HNO_3 + 2NO + H_2O$. This led us to verify the catalytic activity of **1** toward the electro-reduction of NO. The electrocatalytic reduction of NO by **1** starts at a potential value far more positive than that of NO_3^-, with the onset potential difference being on the order of 0.84 V in favor of NO. It may be concluded, then, that the reduction of nitrate ions goes well beyond the formation of NO.

CONCLUSIONS

We have succeeded in preparing the 14-iron(III)-containing, tetrameric heteropolytungstate assemblies, the Wells-Dawson-based 60-tungsto-8-phosphate $[Fe_{14}O_6(OH)_{13}(P_2W_{15}O_{56})_4]^{31-}$

DOI: 10.1021/acs.inorgchem.5b00124
Inorg. Chem. 2015, 54, 6136−6146

(**1**), and the Keggin-based 36-tungsto-4-silicate $[Na_2Fe_{14}(OH)_{12}(PO_4)_4(A\text{-}\alpha\text{-}SiW_9O_{34})_4]^{20-}$ (**2**), as well as the isostructural 36-tungsto-4-germanate $[Na_2Fe_{14}(OH)_{12}(PO_4)_4(A\text{-}\alpha\text{-}GeW_9O_{34})_4]^{20-}$ (**3**) tetrameric assemblies with distinctly different stereochemistries for the Fe_{14} clusters (**1** compared to **2** and **3**). These polyanions were synthesized by interaction of different iron salts with the trilacunary Wells−Dawson precursor $[P_2W_{15}O_{56}]^{12-}$ (**1**) or the trilacunary Keggin precursors $[A\text{-}\alpha\text{-}XW_9O_{34}]^{10-}$ (X = Si, **2**; Ge, **3**) in the presence of acetate (**1**) or phosphate (**2, 3**) in aqueous solution using conventional conditions. The hydrated salts of **1**−**3** were characterized in the solid state by single-crystal X-ray diffraction, infrared spectroscopy, thermogravimetric and elemental analysis, and magnetic susceptibility measurements. The electrochemical properties of these compounds in the solution state were also investigated. Magnetic studies revealed dominant antiferromagnetic interactions among the iron(III) ions in polyanions **1**−**3**. Although it was not possible to propose a quantitative estimate for the exchange interactions, from the structures it is clear that multiple and complex interaction pathways are present due to the high nuclearity of the iron-oxo clusters. The electrochemical studies revealed that the Fe^{III} centers are electroactive, giving rise to a 14-electron (per molecule of **1**) reduction wave preceding those associated with the W centers, at pH 5. Three reversible reduction waves, at relatively high potentials, are observed when **1** is tested at pH 2, meaning that the apparent equivalence of the Fe^{III} centers observed at pH 5 is lost at a higher H^+ concentration. The capability of exchanging several electrons at favorable potentials renders **1** a potential candidate for electrocatalytic processes. It turns out to be effective for the electrocatalytic reduction of O_2, H_2O_2, NO_3^-, and NO. Our ongoing research demonstrates the important role of pH and coligands during the formation of transition metal-containing POMs, which allowed us to isolate novel discrete polynuclear 3d-metal-containing magnetic POMs. Currently we use this approach to prepare other examples of such a POM family, including mixed-valence systems.

■ ASSOCIATED CONTENT

Supporting Information

Infrared spectra, thermograms, and electrochemistry data for **1**−**3**, as well as crystallographic data in CIF format. The Supporting Information is available free of charge on the ACS Publications website at DOI: 10.1021/acs.inorgchem.5b00124.

■ AUTHOR INFORMATION

Corresponding Authors

*E-mail: u.kortz@jacobs-university.de. Fax: +49-421-200 3102. Phone: +49-421-200 3235.

*E-mail: israel.mbomekalle@u-psud.fr. Fax: +33 1 69 15 61 88. Phone: +33 1 69 15 41 59.

*E-mail: annie.powell@kit.edu. Fax: +49 721-608-48142. Phone: +49 721-608-42135.

Present Address

$^{\nabla}$(M.I.) Institute of Nanotechnology, Karlsruhe Institute of Technology (KIT), Hermann-von-Helmholtz Platz 1, 76344 Eggenstein-Leopoldshafen, Germany.

Author Contributions

M.I., A.H., and Y.X. contributed equally.

Notes

The authors declare no competing financial interest.

■ ACKNOWLEDGMENTS

U.K. thanks Jacobs University and the German Science Foundation (DFG KO-2288/20-1) for research support, and also acknowledges the COST Action CM1203 (PoCheMoN). M.I. thanks DFG and Institute of Nanotechnology, Karlsruhe Institute of Technology (KIT), for a postdoctoral fellowship. She also thanks the University of Balochistan, Quetta, Pakistan, for allowing her to pursue her Ph.D. and postdoctoral work at Jacobs University and KIT, respectively. A.H. thanks the German Academic Exchange Council (DAAD) for a Ph.D. fellowship. Y.X. acknowledges an M.S. fellowship from the Jacobs University Nanofun Research Center. V.M. and A.K.P. acknowledge support from the CFN. I.M.M. and P.d.O. acknowledge support from the Université Paris-Sud and the Centre National de la Recherche Scientifique (CNRS). Figures 1−6 were generated by *Diamond*, Version 3.2 (copyright Crystal Impact GbR), and Figure 7 by CrystalMaker, Version 2.5.5.

■ REFERENCES

(1) (a) Pope, M. T. *Heteropoly and Isopoly Oxometalates*; Springer: Berlin, 1983. (b) Pope, M. T.; Müller, A. *Angew. Chem., Int. Ed. Engl.* **1991**, *30*, 34−48. (c) Hill, C. L.; Prosser-McCartha, C. M. *Coord. Chem. Rev.* **1995**, *143*, 407−455. (d) *Chem. Rev.* Hill, C. L., Special Issue Ed.; **1998**, *98*, 1−2. (e) Müller, A.; Roy, S. *Coord. Chem. Rev.* **2003**, *245*, 153−166. (f) Cronin, L. In *Comprehensive Coordination Chemistry II*; McCleverty, J. A., Meyer, T. J., Eds.; Elsevier: Amsterdam, 2004; Vol. *7*; pp 1−56. (g) Hasenknopf, B.; Micoine, K.; Lacôte, E.; Thorimbert, S.; Malacria, M.; Thouvenot, R. *Eur. J. Inorg. Chem.* **2008**, 5001−5013. (h) Kortz, U.; Müller, A.; van Slageren, J.; Schnack, J.; Dalal, N. S.; Dressel, M. *Coord. Chem. Rev.* **2009**, *253*, 2315−2327. (i) *Eur. J. Inorg. Chem.* Issue Dedicated to Polyoxometalates; Kortz, U., Guest Ed.; **2009**, *34*. (j) Long, D. L.; Tsunashima, R.; Cronin, L. *Angew. Chem., Int. Ed.* **2010**, *49*, 1736−1758. (k) Izarova, N. V.; Pope, M. T.; Kortz, U. *Angew. Chem., Int. Ed.* **2012**, *51*, 9492−9510. (l) Clemente-Juan, J. M.; Coronado, E.; Gaita-Ariño, A. *Chem. Soc. Rev.* **2012**, *41*, 7464−7478. (m) Lv, H.; Geletii, Y. V.; Zhao, C.; Vickers, J. W.; Zhu, G.; Luo, Z.; Song, J.; Lian, T.; Musaev, D. G.; Hill, C. L. *Chem. Soc. Rev.* **2012**, *41*, 7572−7589. (n) Pope, M. T.; Kortz, U. Polyoxometalates. *Encyclopedia of Inorganic and Bioinorganic Chemistry*; John Wiley & Sons, Ltd.: Hoboken, NJ, 2012. (o) *Eur. J. Inorg. Chem.* Cluster Issue Dedicated to Polyoxometalates; Kortz, U., Liu, T., Guest Eds.; **2013**, 7325−7648.

(2) (a) Contant, R.; Tézé, A. *Inorg. Chem.* **1985**, *24*, 4610−4614. (b) *Inorganic Syntheses*; Ginsbergh, A. P., Ed.; Wiley: New York, **1990**, *27*, 85−111. (c) Haraguchi, N.; Okaue, Y.; Isobe, T.; Matsuda, Y. *Inorg. Chem.* **1994**, *33*, 1015−1020.

(3) (a) Zimmermann, M.; Belai, N.; Butcher, R. J.; Pope, M. T.; Chubarova, E. V.; Dickman, M. H.; Kortz, U. *Inorg. Chem.* **2007**, *46*, 1737−1740. (b) Ritchie, C.; Streb, C.; Thiel, J.; Mitchell, S. G.; Miras, H. N.; Long, D.-L.; Boyd, T.; Peacock, R. D.; McGlone, T.; Cronin, L. *Angew. Chem., Int. Ed.* **2008**, *47*, 6881−6884. (c) Wu, Q.; Li, Y.-G.; Wang, Y.-H.; Wang, E.-B.; Zhang, Z.-M.; Clérac, R. *Inorg. Chem.* **2009**, *48*, 1606−1612. (d) Bassil, B. S.; Ibrahim, M.; Mal, S. S.; Suchopar, A.; Ngo Biboum, R.; Keita, B.; Nadjo, L.; Nellutla, S.; van Tol, J.; Dalal, N. S.; Kortz, U. *Inorg. Chem.* **2010**, *49*, 4949−4959. (e) Assran, A. S.; Izarova, N. V.; Kortz, U. *CystEngComm* **2010**, *12*, 2684−2686. (f) Bassil, B. S.; Ibrahim, M.; Al-Oweini, R.; Asano, M.; Wang, Z.; van Tol, J.; Dalal, N. S.; Choi, K.-Y.; Biboum, R. N.; Keita, B.; Nadjo, L.; Kortz, U. *Angew. Chem., Int. Ed.* **2011**, *50*, 5961−5964. (g) Cong, S.; Yan, L. K.; Wen, S. Z.; Guan, W.; Su, Z. M. *Theor. Chem. Acc.* **2011**, *130*, 1043−1053. (h) Ismail, A. H.; Bassil, B. S.; Yassin, G. H.; Keita, B.; Kortz, U. *Chem.—Eur. J.* **2012**, *18*, 6163−6166. (i) Al-Oweini, R.; Sartorel, A.; Bassil, B. S.; Natali, M.; Berardi, S.; Scandola, F.; Kortz, U.; Bonchio, M. *Angew. Chem., Int. Ed.* **2014**, *53*, 11182−11185. (j) Jiao, Y. Q.; Qin, C.; Wang, X. L.; Liu, F. H.; Huang, P.; Wang, C. G.; Shao, K. Z.; Su, Z. M. *Chem. Commun.* **2014**, *50*, 5961−5963. (k) Han, X. B.; Zhang, Z.-M.; Zhang, T.; Li, Y. G.; Lin, W.; You, W.; Su, Z.-M.; Wang, E. B. *J. Am. Chem. Soc.* **2014**, *136*, 5359−5366.

DOI: 10.1021/acs.inorgchem.5b00124
Inorg. Chem. 2015, 54, 6136−6146

(4) (a) Zheng, S.-T.; Yang, G.-Y. *Chem. Soc. Rev.* **2012**, *41*, 7623−7646. (b) Oms, O.; Dolbecq, A.; Mialane, P. *Chem. Soc. Rev.* **2012**, *41*, 7497−7536.
(5) (a) Kurtz, D. M. *Chem. Rev.* **1990**, *90*, 585−606. (b) Christou, G.; Gatteschi, D.; Hendrickson, D. N.; Sessoli, R. *MRS Bull.* **2000**, *25*, 66−71. (c) Gatteschi, D.; Sessoli, R. *Angew. Chem., Int. Ed.* **2003**, *42*, 268−297. (d) Botar, B.; Geletii, Y. V.; Kögerler, P.; Musaev, D. G.; Morokuma, K.; Weinstock, I. A.; Hill, C. L. *J. Am. Chem. Soc.* **2006**, *128*, 11268−11277. (e) Theil, E. C.; Matzapetakis, M.; Liu, X. *J. Biol. Inorg. Chem.* **2006**, *11*, 803−810. (f) Compain, J.-D.; Mialane, P.; Dolbecq, A.; Mbomekallé, I. M.; Marrot, J.; Sécheresse, F.; Riviére, E.; Rogez, G.; Wernsdorfer, W. *Angew. Chem., Int. Ed.* **2009**, *48*, 3077−3081.
(6) (a) Müller, A.; Sarkar, S.; Shah, S. Q. N.; Bögge, H.; Schmidtmann, M.; Sarkar, Sh.; Kögerler, P.; Hauptfleisch, B.; Trautwein, A. X.; Schünemann, V. *Angew. Chem., Int. Ed.* **1999**, *38*, 3238−3241. (b) Mbomekallé, I. M.; Keita, B.; Nadjo, L.; Berthet, P.; Hardcastle, K. I.; Hill, C. L.; Anderson, T. M. *Inorg. Chem.* **2003**, *42*, 1163−1169. (c) Bi, L.; Kortz, U.; Nellutia, S.; Stowe, A. C.; van Tol, J.; Dalal, N. S.; Keita, B.; Nadjo, L. *Inorg. Chem.* **2005**, *44*, 896−903. (d) Anderson, T. M.; Cao, R.; Wade, A. N.; Hardcastle, K. I.; Hill, C. L.; Ammam, M.; Keita, B.; Nadjo, L. *Eur. J. Inorg. Chem.* **2005**, 1770−1775. (e) Godin, B.; Chen, Y.; Vaissermann, J.; Ruhlmann, L.; Verdaguer, M.; Gouzerh, P. *Angew. Chem., Int. Ed.* **2005**, *44*, 3072−3075. (f) Mal, S. S.; Dickman, M. H.; Kortz, U.; Todea, A. M.; Merca, A.; Bögge, H.; Glaser, T.; Müller, A.; Nellutla, S.; Kaur, N.; van Tol, J.; Dalal, N. S.; Keita, B.; Nadjo, L. *Chem.—Eur. J.* **2008**, *14*, 1186−1195. (g) Zhao, J.-W.; Jia, H.-P.; Zhang, J.; Zheng, S.-T.; Yang, G.-Y. *Chem.−Eur. J.* **2007**, *13*, 10030−10045. (h) Zhao, J.; Zhang, J.; Zheng, S.; Yang, G. *Inorg. Chem.* **2007**, *46*, 10944−10946. (i) Pradeep, C. P.; Long, D.; Kögerler, P.; Cronin, L. *Chem. Commun.* **2007**, 4254−4256. (j) Pichon, C.; Dolbecq, A.; Mialane, P. R.; Marrot, J.; Rivière, E.; Sécheresse, F. *Dalton Trans.* **2008**, 71−76. (k) Chen, W.; Li, Y.; Wang, Y.; Wang, E.; Zhang, Z. *Z. Anorg. Allg. Chem.* **2009**, *635*, 1678−1687. (l) Molina, I. M.; Miras, H. N.; Long, D. L.; Cronin, L. *Dalton Trans.* **2014**, *43*, 5190−5199. (m) Winter, R. S.; Cameron, J. M.; Cronin, L. *J. Am. Chem. Soc.* **2014**, *136*, 2753−12761.
(7) (a) Bassil, B. S.; Nellutla, S.; Kortz, U.; Stowe, A. C.; van Tol, J.; Dalal, N. S.; Keita, B.; Nadjo, L. *Inorg. Chem.* **2005**, *44*, 2659−2665. (b) Mal, S. S.; Kortz, U. *Angew. Chem., Int. Ed.* **2005**, *44*, 3777−3780. (c) Pichon, C.; Mialane, P.; Dolbecq, A.; Marrot, J.; Rivière, E.; Bassil, B. S.; Kortz, U.; Keita, B.; Nadjo, L.; Sécheresse, F. *Inorg. Chem.* **2008**, *47*, 11120−11645. (d) Mal, S. S.; Bassil, B. S.; Ibrahim, M.; Nellutla, S.; van Tol, J.; Dalal, N. S.; Fernández, J. A.; López, X.; Poblet, M. J.; Ngo Biboum, R.; Keita, B.; Kortz, U. *Inorg. Chem.* **2009**, *48*, 11636−11645. (e) Ibrahim, M.; Lan, Y.; Bassil, B. S.; Xiang, Y.; Suchopar, A.; Powell, A. K.; Kortz, U. *Angew. Chem., Int. Ed.* **2011**, *50*, 4708−4711. (f) Ibrahim, M.; Xiang, Y.; Bassil, B. S.; Lan, Y.; Powell, A. K.; de Oliveira, P.; Keita, B.; Kortz, U. *Inorg. Chem.* **2013**, *52*, 8399−8408. (g) Ibrahim, M.; Haider, A.; Lan, Y.; Bassil, B. S.; Carey, A. M.; Liu, R.; Zhang, G.; Keita, B.; Li, W.; Kostakis, G. E.; Powell, A. K.; Kortz, U. *Inorg. Chem.* **2014**, *53*, 263−266.
(8) Zhang, Z. M.; Li, Y. G.; Yao, S.; Wang, E. B.; Wang, Y. H.; Clérac, R. *Angew. Chem., Int. Ed.* **2009**, *48*, 1581−1584.
(9) Zhang, Z.-M.; Yao, S.; Li, Y.-G.; Clérac, R.; Lu, Y.; Su, Z.-M.; Wang, E.-B. *J. Am. Chem. Soc.* **2009**, *131*, 14600−14601.
(10) (a) Hervé, G.; Tézé, A. *Inorg. Chem.* **1977**, *16*, 2115−2117. (b) Finke, R. G.; Droege, M. W.; Domaille, P. J. *Inorg. Chem.* **1987**, *26*, 3886−3896. (c) Laronze, N.; Marrot, J.; Hervé, G. *Inorg. Chem.* **2003**, *42*, 5857−5862.
(11) *SAINT*; Bruker AXS Inc.: Madison, WI, 2007.
(12) (a) Sheldrick, G. M. *SADABS*; University of Göttingen: Göttingen, Germany, 1996. (b) Sheldrick, G. M. *Acta Crystallogr., Sect. A* **2007**, *64*, 112−122.
(13) Sheldrick, G. M. *SHELX-97, Program for Solution of Crystal Structures*; University of Göttingen: Göttingen, Germany, 1997.
(14) Vila, N.; Aparicio, P. A.; Sécheresse, F.; Poblet, J. M.; López, X.; Mbomekalle, I. M. *Inorg. Chem.* **2012**, *51*, 6129−6138.
(15) (a) Brown, I. D. *Acta Crystallogr., Sect. B* **1992**, *48*, 553−572. (b) Burdett, J. K.; Hawthorne, F. C. *Am. Mineral.* **1993**, *78*, 884−892. (c) Brown, I. D. *Acta Crystallogr., Sect. B* **1997**, *53*, 381−393. (d) Wood, R. M.; Palenik, G. J. *Inorg. Chem.* **1998**, *37*, 4149.
(16) (c) Kostakis, G. E.; Blatov, V. A.; Proserpio, D. M. *Dalton Trans* **2012**, *41*, 4634−4640.
(17) Cronin, L.; Fielden, J. Coordination Clusters. In *Encyclopedia of Supramolecular Chemistry*; Taylor and Francis: London, 2007; pp 1−10.
(18) Kostakis, G. E.; Powell, A. K. *Coord. Chem. Rev.* **2009**, *253*, 2686−2697.
(19) Langley, S. K.; Moubaraki, B.; Berry, K. J.; Murray, K. S. *Dalton Trans.* **2010**, *39*, 4848−4855.
(20) Xiang, H.; Mereacre, V.; Lan, Y.; Lu, T.-B.; Anson, C. E.; Powell, A. K. *Chem. Commun.* **2013**, *49*, 7385−7387.
(21) Song, W.; Wang, X.; Liu, Y.; Liu, J.; Xu, H. J. *Electroanal. Chem.* **1999**, *476*, 85−89.
(22) Keita, B.; Mbomekallé, I. M.; Nadjo, L.; Anderson, T. M.; Hill, C. L. *Inorg. Chem.* **2004**, *43*, 3257−3263.
(23) Hill, C. L.; Weinstock, I. A. *Nature* **1997**, *388*, 332−333.
(24) CPC carried out at a potential of E_c = +0.26 V vs SCE at pH 2 showed that the first wave corresponded to the reduction of at least 5 Fe^{III} centers over the 14 present.
(25) Keita, B.; Mbomekallé, I. M.; Lu, Y. W.; Nadjo, L.; Berthet, P.; Anderson, T. M.; Hill, C. L. *Eur. J. Inorg. Chem.* **2004**, 3462−3475.
(26) Keita, B.; Nadjo, L. Electrochemistry of Polyoxometalates. *Encyclopedia of Electrochemistry*; Bard, A. J., Stratmann, M., Eds.; Wiley-VCH: New York, 2006; Vol 7, pp 607−700.
(27) Andrieux, C. P.; Dumas-Bouchiat, J. M.; Savéant, J. M. *J. Electroanal. Chem.* **1980**, *113*, 1−18.
(28) Toth, J. E.; Anson, F. C. *J. Am. Chem. Soc.* **1989**, *256*, 361−370.
(29) (a) Keita, B.; Nadjo, L., Contant, R.; Fournier, M.; Hervé, G. (CNRS) French Patent 89/1, 728, 1989. (b) Keita, B.; Nadjo, L., Contant, R.; Fournier, M.; Hervé, G. (CNRS) Eur. Patent App EP 382, 644, 1990. (c) Keita, B.; Nadjo, L.; Contant, R.; Fournier, M.; Hervé, G. *Chem. Abstr.* **1991**, *114*, 191882u.

DOI: 10.1021/acs.inorgchem.5b00124
Inorg. Chem. 2015, 54, 6136−6146